Synthesis, characterization and cytotoxicity of S-nitroso-mercaptosuccinic acid-containing alginate/chitosan nanoparticles

IOP Conf. Series: Journal of Physics: Conf. Series **838** (2017) 012032 doi:10.1088/1742-6596/838/1/012032

Synthesis, characterization and cytotoxicity of S-nitroso-mercaptosuccinic acid-containing alginate/chitosan nanoparticles

Amedea B. Seabra[1,2*] Giulia K. Fabbri[2], Milena T. Pelegrino[1,2], Letícia C. Silva[1], Tiago Rodrigues[1]

[1]Center of Natural and Human Sciences, Universidade Federal do ABC, Av. dos Estados 5001, CEP 09210-580, Santo André, SP, Brazil.
[2]Exact and Earth Sciences Department, Universidade Federal de São Paulo, Rua São Nicolau, 210, CEP 09913-030, Diadema, SP, Brazil

*amedea.seabra@ufabc.edu.br

Abstract. Nitric oxide (NO) is an endogenous free radical, which plays key roles in several biological processes including vasodilation, neurotransmission, inhibition of platelet adhesion, cytotoxicity against pathogens, wound healing, and defense against cancer. Due to the relative instability of NO *in vivo* (half-life of *ca*. 0.5 seconds), there is an increasing interest in the development of low molecular weight NO donors, such as S-nitrosothiols (RSNOs), which are able to prolong and preserve the biological activities of NO *in vivo*. In order to enhance the sustained NO release in several biomedical applications, RSNOs have been successfully allied to nanomaterials. In this context, this work describes the synthesis and characterization of the NO donor S-nitroso-mercaptosuccinic acid (S-nitroso-MSA), which belongs to the class of RSNOs, and its incorporation in polymeric biodegradable nanoparticles composed by alginate/chitosan. First, chitosan nanoparticles were obtained by gelation process with sodium tripolyphosphate (TPP), followed by the addition of the alginate layer, to enhance the nanoparticle protection. The obtained nanoparticles presented a hydrodynamic diameter of 343 ± 38 nm, polydispersity index (PDI) of 0.36 ± 0.1, and zeta potential of – 30.3 ± 0.4 mV, indicating their thermal stability in aqueous suspension. The negative zeta potential value was assigned to the presence of alginate chains on the surface of chitosan/TPP nanoparticles. The encapsulation efficiency of the NO donor into the polymeric nanoparticles was found to be 98 ± 0.2%. The high encapsulation efficiency value was attributed to the positive interactions between the NO donor and the polymeric content of the nanoparticles. Kinetics of NO release from the nanoparticles revealed a spontaneous and sustained release of therapeutic amounts of NO, for several hours under physiological temperature. The incubation of NO-releasing alginate/chitosan nanoparticles with human hepatocellular carcinoma (HepG2) cell line revealed a concentration-dependent toxicity. These results point to the promising uses of NO-releasing alginate/chitosan nanoparticles for anti-cancer chemotherapy.

1. Introduction

Polymeric nanoparticles composed by polysaccharides have been extensively studied due to their interesting properties such as biocompatibility and biodegradability [1]. Chitosan (CS) is on the most employed biopolymer in pharmacological and biomedical applications, in the forms of films, gels,

micro and nanoparticles [2]. Alginate (ALG) is naturally occurring polysaccharide extracted from brown seaweed. It is composed of two types of uronic acids, alfa-*L*-gluronic acid and beta-*D*-manuronic acid, which contributes for the bioadhesiveness and drug-binding properties of this polymer [3]. ALG can interact with calcium inducing gel formation [4], and may also form complexes with polycations, CS or peptides [5].

Nitric oxide (NO) is an important endogenous molecule, which plays several physiological and pathophysiological functions [1,6-8]. Among them, NO has toxicity towards cancer cells, depending on its concentration [9]. NO is a free radical and relatively instable in the biological medium. S-nitrosothiols (RSNOs) are an important class of NO donors, acting as NO carriers able to spontaneous release free NO [10]. Recently, RSNOs have been incorporated into nanomaterials to enhance the sustained NO release in biomedical applications [1].

The objective of this study was to describe the synthesis, characterization and cytotoxicity of CS nanoparticles containing the NO donor S-nitroso-mercaptosuccinic acid (S-nitroso-MSA), which belongs to the class of RSNOs [1,8]. ALG was added onto the surface of CS NPs, leading to the formation of S-nitroso-MSA-CS/ALG NPs (Figure 1).

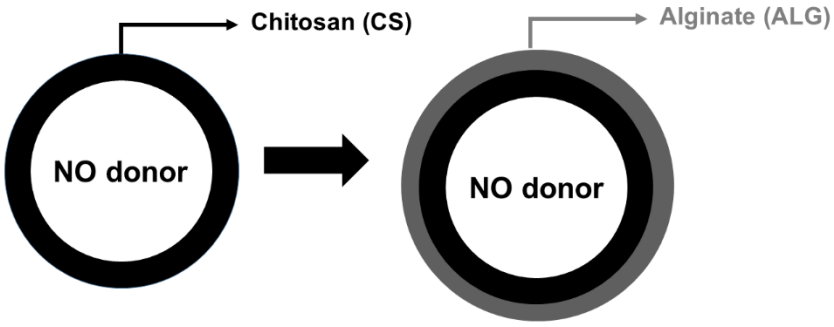

Figure 1. Schematic representation of the synthesized nanoparticles. ALG layer (grey circle) was added on the surface of CS NPs (black circle) containing the NO donor.

ALG is known to increase the mechanical properties of a biomaterial, and also to enhance the stability of encapsulated drugs decreasing the nanoparticle degradation in acid environment or minimizing the degradation actions of hydrolytic enzymes [11]. Moreover, both CS and ALG are mucoadhesive polymers, enhancing the delivery of therapeutic drugs to the mucus layers [12].

In this study, polymeric nanoparticles made of CS and ALG were evaluated regarding their size, stability and potential as drug delivery system, further, the cytotoxicity of the NO-releasing polymeric nanoparticles was demonstrated towards human hepatocellular carcinoma (HepG2) cell line. The results suggest the potential uses of this nanomaterial against cancer cells.

2. Methods

2.1. Synthesis of MSA-CS/ALG NPs

Firstly, CS NPs were synthesized by ionotropic gelation with sodium tripolyphosphate (TPP), as previous described [13]. Briefly, CS (2.6 $mg \cdot mL^{-1}$) and MSA (133.3 $mmol \cdot L^{-1}$) were mixed through magnetic stirring in an aqueous solution of acetic acid (0.175 $mol \cdot L^{-1}$) for 90 min. TPP aqueous solution (0.6 $mg \cdot mL^{-1}$) was added dropwise to the CS/MSA suspension, following the volumetric proportion of 3CS/MSA : 1TPP. The mixture was stirred for further 45 minutes at room temperature leading to the formation of aqueous suspension of CS NPs containing MSA, henceforth, referred as MSA-CS NPs. In a second step, the ALG layer was inserted onto the MSA-CS NPs, as previous

described [14]. Under magnetic stirring and at room temperature, ALG solution (1 $mg \cdot mL^{-1}$) was dropwise in the previous prepared MSA-CS NPs dispersion, following the volumetric proportion of 1ALG: 1 MSA-CS NPs. The final mixture was stirred for further 30 min at room temperature forming a dispersion of MSA-CS/ALG NPs in which the MSA concentration is 50 $mmol \cdot L^{-1}$, showed in Figure 1, and referred as MSA-CS/ALG NPs.

2.2. Dynamic light scattering measurements (DLS)

The hydrodynamic size diameter, polydispersity index (PDI), and zeta potential of MSA-CS/ALG NPs were evaluated by DLS (Nano ZS Zetasizer, Malvern Instruments Co, UK.) [15]. Measurements were performed at a fixed angle of 173°, using a disposable capillary cuvette (DTS1070) after a dilution of 1:10. The results were reported as an average of three independent experiments with the error bar values expressed by their standard error of the mean (SEM).

2.3. Encapsulation efficiency of MSA into CS/ALC NPs

The encapsulation efficiency of MSA in CS/ALG NPs was measured by the titration of free thiols groups in the MSA structure with the thiol reagent 5,50-dithiobis-(2-nitrobenzoic acid) (DTNB), as already described [16]. Non-encapsulated (free) MSA was separated from encapsulated MSA by using a Microcon centrifugal filter device (MWCO 10,000, Millipore) and titrated with DTNB. The absorption band at 412 nm (ε = 14.15 $mmol^{-1}Lcm^{-1}$), assigned to the formation of 2-nitro-5-thiobenzoate anion that is generated in the reaction of DTNB with MSA, was measured in the ultra violet-visible spectrophotometer (Agilent 8453, Palo Alto, CA, USA). The analysis was performed in duplicates. The percentage of MSA encapsulation was determined by the described equation:

$$(\%) = (\text{mass of MSA encapsulated/mass of MSA total}) \times 100 \quad \text{(Eq. 1)}$$

2.4. Nitrosation of MSA incorporated into CS/ALG NPs

Free thiol group of MSA encapsulated into CS/ALG NPs was nitrosated by the addition of equimolar amount of sodium nitrite ($NaNO_2$, 50 $mmol \cdot L^{-1}$) to the aqueous suspension of MSA-CS/ALG NPs (pH ~4.0). The final suspension was stirred for 30 min in an ice bath (5°C), protected from the ambient light, leading to the formation of S-nitroso-MSA-CS/ALG NPs. The confirmation of the nitrosation of MSA yielding S-nitroso-MSA was performed by the appearance of the characteristic S-NO group absorption bands at 336 nm (ε = 980.0 $mol^{-1} \cdot L \cdot cm^{-1}$) or at 545 nm ($\varepsilon$ = 18.4 $mol^{-1} \cdot L \cdot cm^{-1}$) by using the UV–vis spectrophotometer (Agilent 8453, Palo Alto, CA, USA).

2.5. NO release profile from S-nitroso-MSA-CS/ALG NPs at physiological temperature

The kinetics of NO release from S-nitroso-MSA-CS/ALG NPs was determined by monitoring the spectral changes at 545 nm ($nN \rightarrow \pi^*$ transition) [15,17]. The decay of this absorption band is associated with the decomposition of S-nitroso-MSA with free NO release. The initial concentration of S-nitroso-MSA in the CS/ALG NPs was 50 $mmol \cdot L^{-1}$ and the kinetic data were collected in 30 min intervals at 37ºC for 6 h of monitoring. The amount of S-nitroso-MSA decomposed is related to the amount of NO released, since the decay of the absorption band at 545 nm over time is solely assigned to the cleavage of the S–N bond and NO release. Each point in the kinetic curves represents the average of two independent experiments, with the error bar values expressed by their standard error of the mean (SEM). In order to investigate the mechanism of NO release from S-nitroso-MSA-CS/ALG NPs, the Higuchi model was applied to kinetic curve [18-20]. According to the Higuchi model, the drug release is dependent of the square-root of time, as shown in Eq. 2, where Q_T is the amount of drug released at time t, K_H is the Higuchi dissolution constant and t is time. The results were adjusted through linear regression and the correlation coefficient (R^2) was analyzed [21].

$$Q_t = K_H t^{-0.5} \quad \text{(Eq. 2)}$$

2.6. Cytotoxicity of S-nitroso-MSA-CS/ALG NPs

The cytotoxicity of S-nitroso-MSA-CS/ALG NPs was evaluated towards human hepatocellular carcinoma (HepG2) cell line. Different concentrations of S-nitroso-MSA-CS/ALG NPs and MSA-CS/ALG NPs (control group) were added to each well containing the cells followed by incubation for 24 h at 37°C in a 5% CO_2 atmosphere. After, 3-(4,5-dimethylthiazol-2-Yl)-2,5-diphenyltetrazolium bromide (MTT) solution (0.25 $mg \cdot mL^{-1}$) was added to each well followed by 4 h incubation. Then, 0.1 mL of 10% SDS (prepared in 10 $mmol \cdot L^{-1}$ HCl) was added and incubated overnight to dissolve the formazan crystals, and the plates were read at 570 nm with 630 nm (BiochromAsys Expert Plus Microplate Reader, Biochrom Ltd., UK). The control was performed in the absence of NPs and considered as 100%. Each point represents the average of two independent experiments, with the error bar values expressed by their standard error of the mean (SEM).

3. Results and Discussion

This main objective of this study was to obtain a polymeric NP able to carry and to deliver therapeutic amounts of NO for biomedical applications. To this end, this study reports the preparation of NO-releasing CS based NPs, their characterization, the evaluation of the NO release profile from the NPs and the cytotoxicity of the NPs towards HepG2 cell line. The following sub-sections summarize the main results.

3.1. Synthesis and characterization of MSA-CS/ALG NPs

Polymeric NPs based on CS and/or ALG have been broadly studied and employed as drug delivery system due to their unique chemical and biological properties, such as, mucoadhesiveness, biocompatibility, biodegradability, and non-toxicity [14,19,22]. Indeed, synthesis of CS NPs followed by the addition of ALG layer is able to promote sustained release of encapsulated drugs in a more efficacy manner in comparison with NPs comprised by only CS or ALG [22]. In this study, CS NPs were initially synthesized by the ionotropic gelation method, in which cationic chitosan chains readily interacts with the counter negatively charge TPP ions leading to the formation of the CS NP. This process is based on the interaction of cationic CS chains with multivalent counter ions resulting in the intermolecular and/or intramolecular network structure maintained by ionic interactions between NH_3^+ protonated groups of CS and negatively charged counter ions of TPP. This cross linking leads to the formation of CS NPs. Encapsulation of MSA into CS NPs is performed by the strong electrostatic interactions between MSA and the CS chains. In a second step, addition ALG layers were added on the surface of MSA-CS NPs, leading to the formation of MSA-CS/ALG NPs. The presence of ALG is responsive to confer protection to MSA-CS NPs, which might decrease the degradation rates of NP in biological medium, and therefore protecting the NO donor.

DLS measurements revealed that the hydrodynamic diameter of MSA-CS/ALG NPs was found to be 343 ± 38 nm with a moderate polydispersity index (PDI) of 0.36 ± 0.10. These results are in accordance Biswas and co-workers who reported a hydrodynamic diameter of 432 ± 52 nm and PDI value of 0.368 ± 0.06 for CS/ALG NPs containing antigens [14]. In addition, Costa and co-works reported the hydrodynamic diameter in the rage of 380-420 nm for CS/ALG NPs containing antibiotics [22].

The zeta potential value for MSA-CS/ALG NPs was found to be -30.3 ± 0.4 mV, indicating a moderate stability of the NPs in aqueous environment, which is necessary for biomedical applications. The negative value of the zeta potential confirms the addition of ALG layers on the surface of MSA-CS NPs, since ALG has negative charge due to the presence carboxyl groups. In contrast, a positive zeta potential value of 21.8 ± 1.1 mV was observed for MSA-CS NPs, prior the addition of ALG layers. This positive value is assigned to the presence of protonated amino groups found in CS chains. Our results are in accordance with published papers which report negative values for zeta potential of CS NPs coated with ALG layers, such as -16 to -26 mV for CS/ALG NPs containing paclitaxel [23],

and a zeta potential of *ca.* -38.2 ± 0.3 mV for antibiotic delivery, as reported by Costa and co-workers [22].

The encapsulation efficiency of MSA in CS/ALG NPs was found to be 98.05 ± 0.20 %, indicating a high affinity of MSA to the ALG/CS NPs, as previous described [16]. MSA has positive charge interactions with CS and ALG chains.

3.2 Nitrosation of MSA-CS/ALG NPs leading to the formation of S-nitroso-MSA-CS/ALG NPs

Free thiol groups of MSA-CS/ALG NPs were nitrosated by reacting by nitrous acid (HNO_2) leading to the formation of S-nitroso-MSA-CS/ALG NPs, as shown in Figure 2A. HNO_2 was generated by the presence of sodium nitrite ($NaNO_2$) is acid solution.

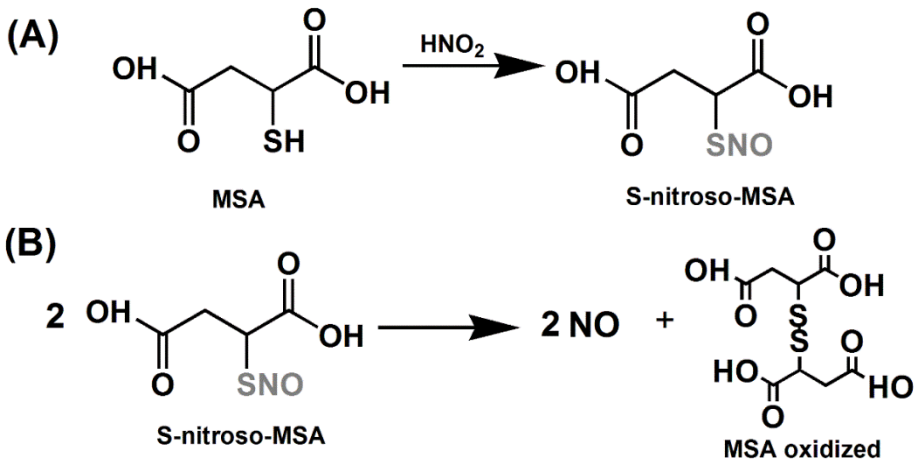

Figure 2. (A) Nitrosation of MSA forming the S-nitroso-MSA which acts as NO donor, (B) S-nitroso-MSA decomposition releasing the free NO yielding oxidized MSA.

3.3. NO release profile from S-nitroso-MSA-CS/ALG NPs at physiological temperature

S-nitroso-MSA is a spontaneous NO donor as shown in Figure 2B. The kinetics of NO release from S-nitroso-MSA-CS/ALG NPs in aqueous solution were monitored by following the spectral changes at 545 nm absorption band, associated the S-N bound cleavage with free NO release (Figure 3) [15, 16,19]. Figure 3 shows that the kinetic curve shows two distinct phases: an initial burst, in the first 2 h, of NO release with the dissolution constant (K_H) of 39.05 ± 1.8 mmol·$Lh^{-0.5}$, followed by a decrease in the rates of NO release from 2 to 6 h. Moreover, the concentration of NO release is in the mmol/L, at this concentration, NO is known to have antitumor and antibacterial activities [24-27]. The NO release from CS/ALG NPs is limited by several mechanisms, such as, diffusion, desorption, particle erosion or the combination of these factors. In order to evaluate the mechanism of NO release from the S-nitroso-MSA-CS/ALG NPs, the Higuchi model was applied to the kinetic curve. The correlation coefficient (R^2) obtained was of 0.981, which indicates that the main mechanism controlling the NO release is the diffusion process over the pores in the polymeric walls. Similar results were reported for the release of NO from CS/ALG NPs [19].

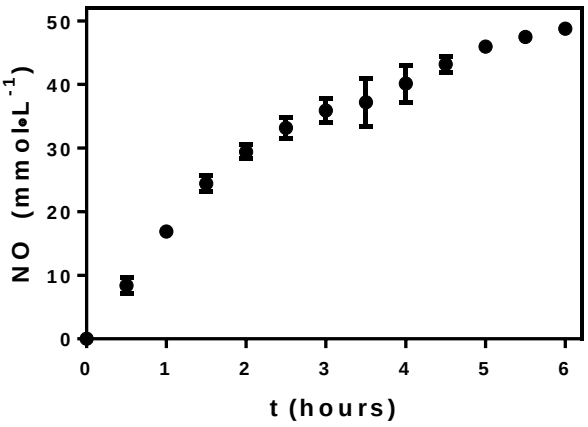

Figure 3. Kinetics of NO release from S-nitroso-MSA-CS/ALG NPs (S-nitroso-MSA concentration of 50 mmol·L^{-1}), at 37°C for 6 h. The results are presented as mean ± standard error of two independent experiments.

3.4. *Cytotoxicity of S-nitroso-MSA-CS/ALG NPs*

Figure 4 shows the viability of HepG2 cells upon treatment with S-nitroso-MSA-CS/ALG NPs and MSA-CS/ALG NPs. For both cases, a decrease in cell viability in a concentration-dependent manner was observed. At 40 µg·mL^{-1}, viability of HepG2 cells decreased to 64.771 ± 7.928% upon incubation with S-nitroso-MSA-CS/ALG NPs. This decrease is *ca*. 22% lower compared to the cell viability upon HepG2 incubation with MSA-CS/ALG NPs at the same concentration.

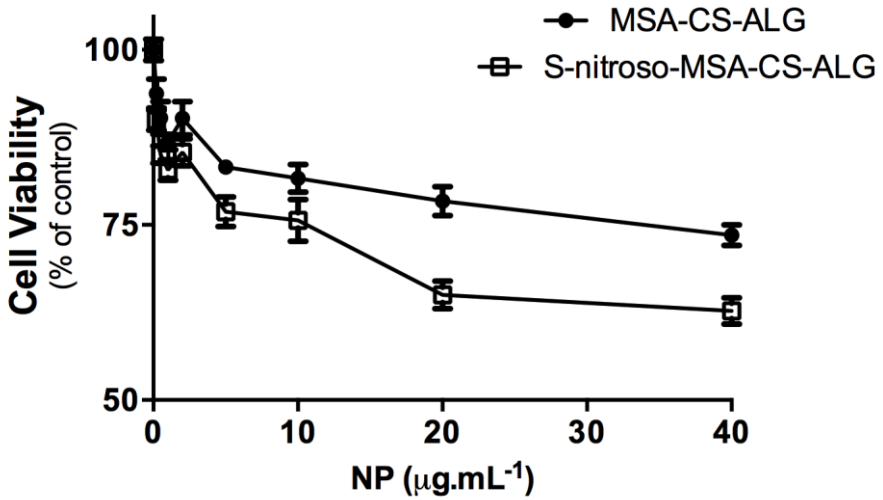

Figure 4. Viability of HepG2 tumor cells upon incubation with S-nitroso-MSA-CS/ALG NPs (empty squares) and MSA-CS/ALG NPs (black circles), at increasing concentrations. Cell viability was estimated by a tetrazolium-based (MTT) reduction assay. The results are presented in percentage of control (absence of NPs) as mean ± standard error of two independent experiments.

It is noteworthy that the polymeric nanoparticle without NO also presented toxicity in HepG2 cells and this toxicity was further increased for the nanoparticle containing the NO donor. This result indicates that NO-releasing CS/ALG NPs presents potential to use against cancer cells.

4. Conclusions

This work describes the synthesis and characterization of NO-releasing CS/ALG NPs. The NO donor S-nitroso-MSA was encapsulated into CS NPs, followed by the addition of ALG layer. This nanoparticle was able to spontaneously release free NO, following the Higuchi mathematical model. The cytotoxicity of S-nitroso-MSA CS/ALG NPs were demonstrated towards HepG2 tumor cell. Further studies to understand the molecular pathways involved in the cytotoxicity of this nanomaterial is under investigation.

Acknowledgements: FAPESP (Proc. 2016/10347-6 and 2016/07367-5), CNPq (Proc. 486067/2013-0) the Brazilian Network on Nanotoxicology (Grant number: 552120/2011-1) (MCTI/CNPq), the Laboratory of Nanostructure Synthesis and Biosystem Interactions-NANOBIOSS (MCTI) (Grant number: 402280-2013), Newton Advanced Fellowship (The Royal Society NA140046).

References

[1] Seabra AB, de Lima R and Calderón M 2015 *Curr. Top. Med. Chem.* **15** 298
[2] Yin L, Su T, Chang J, Liu R, He B and Gu Z 2014 *NANO* **9** 1450075
[3] Markeb AA, El-Maali NA, Sayed DM, Osama A, Abdel-Malek MAY, Zaki AH and Elwanis MEA, Driscoll JJ 2016 *Int. J. Breast Cancer* **2016**
[4] Manuja A, Kumara B, Chopraa M, Bajaja A, Kumara R, Dilbaghib N, Kumarb S, Singha S, Riyesha T and Yadavaa SC 2016 *Int. J. Biol. Macromolec.* **88** 146
[5] Sundar S, Kundu J and Kundu SC 2010 *Sci. Technol. Adv. Mater.* **11** 014104
[6] Basudhar D, Cheng RC, Bharadwaj G, Ridnour LA, Wink DA and Miranda KM 2015 *Free Radic. Biol. Med.* **83** 101
[7] Bonavida B and Garban 2015 *Redox Biol.* **6** 486
[8] Seabra AB, Justo GZ and Haddad PS 2015 *Biotechnol. Adv.* **33** 1370
[9] Burke AJ, Sullivan FJ, Giles FJ and Glynn SA 2013 *Carcinogenesis* **34** 503
[10] de Oliveira MG 2016 *Basic Clin. Pharmacol. Toxicol.* doi: 10.1111/bcpt.12588
[11] Borges O, Cordeiro-da-Silva A, Romeijn SG, Amid M, de Sousa A, Borchard G and Junginger HE 2013 *J. Control. Release* **114** 348
[12] Wu W, Perrin-Sarrado C, Ming H, Lartaud I, Maincent P, Hu X, Sapin-Minet A and Gaucher C 2016 *Nanomedicine* **12** 1795
[13] Pereira AES, Narciso AM, Seabra AB and Fraceto LF 2015 *JPCS* **617** 012025
[14] Biswas S, Chattopadhyay M, Sen KK and Saha MK 2015 *Carbohyd. Polym.* **121** 403
[15] Seabra AB, Kitice NA, Pelegrino MT, Lancheros CAC, Yamauchi LM, Pinge-Filho P and Yamada-Ogatta SF 2015 *JPCS* **617** 012020
[16] Cardozo VF, Lancheros CA, Narciso AM, Valereto EC, Kobayashi RKT, Seabra AB and Nakazato G 2014 *Int. J. Pharm.* **473** 20
[17] de Oliveira MG, Shishido SM, Seabra AB and Morgon NH 2002 *J. Phys. Chem. A* **106** 8963
[18] Grillo R, de Melo NFS, de Araújo SR, de Paula E, Rosa AH, Fraceto LH 2010 *J. Drug Target* **18** 688
[19] Marcato PD, Adami LF, Barbosa RM, Melo PS, Ferreira IS, de Paula L, Durán N and Seabra AB 2013 *Curr. Nanosci.* **9** 1
[20] Kim JO, Noh JK, Thapa RK, Hasan N, Choi M, Kim JH, Lee JH, Ku SK and Yoo JW 2015 *Int. J. Biol. Macromol.* **79** 217
[21] Costa and Lobo 2001 *Eur. J. Pharm. Sci.* **13** 123
[22] Costa JR, Silva NC, Sarmento B and Pintado M 2015 *Eur. J. Clin. Microbio.l Infect. Dis.* **34** 1255
[23] Wang F, Yang S, Yuan J, Gao Q and Huang C 2016 *J. Biomater. Appl.* **23** 619
[24] Quinn JF, Whittaker MR and Davis TP 2015 *J. Control. Release* **205** 190

[25] Backlund CJ, Worley BV and Schoenfisch MH 2015 *Acta Biomater.* **29** 198
[26] de la Rosa AJ, Rodríguez-Hernández A, González R, Romero-Brufau S, Navarro-Villarán E, Barrera-Pulido L and Pereira S 2016 *Gene Ther.* **23** 67
[27] Seabra AB, Pelegrino MT and Haddad PS 2016 Antibiotic Resistance *Can nitric oxide overcome bacterial resistance to antibiotics?* Ed 1 (Elsevier) pp 187-201